Available online at www.sciencedirect.com
ScienceDirect
Journal of Hazardous Materials 147 (2007) 139–147
Journal of Hazardous Materials
www.elsevier.com/locate/jhazmat

Capacity of adsorption of Pb^{2+} and Ni^{2+} from aqueous solutions by chitosan produced from silkworm chrysalides in different degrees of deacetylation

Alexandre T. Paulino [a,*], Marcos R. Guilherme [b], Adriano V. Reis [a], Elias B. Tambourgi [b], Jorge Nozaki [a,✠], Edvani C. Muniz [a]

[a] *Departamento de Química, Universidade Estadual de Maringá, Avenida Colombo 5790, CEP 87020-900, Maringá-PR, Brazil*
[b] *Universidade Estadual de Campinas, Faculdade de Engenharia Química, Departamento de Sistemas Químicos e Informática DESQ, Zeferino Vaz 13081-970, Campinas, SP, Brazil*

Received 7 June 2006; received in revised form 19 December 2006; accepted 22 December 2006
Available online 3 January 2007

Abstract

The binding capacities of chitin (CT) and chitosan (CS) produced from silkworm chrysalides were investigated aiming at their future application in the removal of Pb^{2+} and Ni^{2+} from wastewaters. CS with 75% deacetylation degree (DD) exhibited good binding performance for Pb^{2+}, but bad efficiency for Ni^{2+}. The maximum binding capacity obtained from isotherms for CS–Pb was 141.10 mg g^{-1} and 52.81 mg g^{-1} for CS–Ni. The binding capacities for CT were 32.01 mg g^{-1} for Pb^{2+} and 61.24 mg g^{-1} for Ni^{2+}. The authors attribute these behaviors to two main factors: (i) the large ionic size of Pb^{2+} and (ii) the steric hindrance due to CT acetyl groups. Metal binding onto CS was evaluated by the Freundlich and Langmuir isotherm models. The parameter values obtained from the isotherm analysis confirmed that Pb^{2+} and Ni^{2+} interact differently with CS and that various factors influence their adsorption. Thermogravimetric analysis (TGA) showed that the thermal behavior of CS with 75% deacetylation degree was in the same profile of standard CS; however, the binding of the metals onto its structure affects the curve profile.

Keywords: Silkworm chrysalides; Adsorption; Heavy metals; Chitosan; Deacetylation degree

1. Introduction

Lead (Pb^{2+}) and nickel (Ni^{2+}) are found in low concentrations in some biological systems and high concentrations of these metals are lethal [1–3]. Pb^{2+} is found in air, water, soil, rocks and sediments and it is used in glasses, ceramics, tanned leather, ammunition, and in other types of materials such as metals, tubes, batteries, etc. Furthermore, Pb^{2+} has also been used as a base in different types of inks and many countries have already prohibited its use in domestic inks [4].

Studies have demonstrated that high levels of Ni^{2+} in human hair are associated to cardiovascular problems and immune dysfunction by alteration of immunoglobulin levels [5]. The toxicity of Ni^{2+} has been associated to dermatitis, allergies, renal disturbances, hepatitis, infertility, lung cancer, stomatitis, gingivitis, insomnia and nauseas. These problems are prevented in humans [5] by appropriate levels of Fe^{2+}, Cu^{2+}, Zn^{2+} and Mn^{2+}, which inhibit the absorption and retention of Ni^{2+}.

Low-priced solid adsorbents have been widely applied in wastewater treatment throughout the world [6–9]. These adsorbents are considered inexpensive because they require little processing. Low-cost adsorbents can also be easily found in nature or as industrial sub-products [10]. Examples of low-cost adsorbents found in nature are bark, a waste from the timber industry; lignin, a waste from paper industry; dead biomass such as rice hull, seaweed alginate, xanthate; minerals such as zeolites, clay, fly ash, coal, natural oxides, miscellaneous activated carbon, peat moss, etc. They are widely applied in wastewater treatment as an alternative large scale procedure [11–13]. These absorbents may remove Hg^{2+}, Cd^{2+}, Pb^{2+}, Cr^{6+} and Cr^{3+} metallic ions present in industrial process wastewaters [13,14].

Chitosan, CS, is a copolymer of β-(1,4)-D-glucosamin and β-(1,4)-*N*-acetyl-D-glucosamin. It is a crystalline polysaccharide obtained by deacetylation of the biopolymer chitin, CT. It is widely used due to its biodegradability and nontoxicity. The

* Corresponding author. Tel.: +55 44 3261 4332; fax: +55 44 3261 4125.
E-mail address: atpquim@yahoo.com.br (A.T. Paulino).
✠ In memoriam.

0304-3894/$ – see front matter © 2007 Elsevier B.V. All rights reserved.
doi:10.1016/j.jhazmat.2006.12.059

differences between the structures of CT and CS are just the presence of acetyl in CT and the presence of $-NH_2$ groups in CS. Thus, the $-NH_2$ of CS may interact with metallic ions and studies demonstrate that it is efficient in their adsorption [15,16]. The amine groups in CS possess the best active sites for the formation of complexes with metallic ions, which are stabilized by coordination [17]. The maximum binding capacity of CS to heavy metals may decrease as the amount of acetyl groups in its structure increases. As the adsorption of heavy metals onto CS is stabilized by the interaction between amine groups and metallic cations, it can be considered that when the amount of amine groups decreases, in case of the addition of acetylated composites to the chitosan network, the maximum binding capacity also decreases [17,18]. The CS chains are less flexible after the addition of either acetyl groups or others carboxyl groups. The crosslinking of CS by reaction with glutaraldehyde or other moieties and the presence of acetyl groups will hinder the diffusion of metal ions throughout the network. These effects decrease the capacity of chemically modified CS to remove heavy metals from wastewater and drinking water [18–20].

Silkworm chrysalides (BM), *Bombix Mori*, rejects from silk fiber industries after fiber extraction, are rich in chitin. With the intention of finding an inexpensive and high capacity adsorbent for the removal of Pb^{2+} and Ni^{2+}, we have used CS produced from CT found in BM [17,21]. To this end, it is important to investigate the binding capacity of Pb^{2+} and Ni^{2+} to CS. CS with various degrees of deacetylation have been used in adsorption experiments of Pb^{2+} and Ni^{2+} ions. The binding capacity of these metallic ions to CT, used in this work as a reference, was investigated as well.

2. Materials and methods

2.1. Materials

Silkworm chrysalide samples were kindly supplied by Cocamar (Cooperativa Agroindustrial, Maringá-PR, Brazil). The Pb^{2+} and Ni^{2+} purchased from Merck and used in the adsorption experiments as standards had analytical grade. All other reagents of analytical grade were used without further purification.

2.2. Extraction of CT from BM

BM were dried by lyophilization (Martin Christ, Freeze Dryer, Alpha 1–2/LD) for 12 h, reduced to powder with a knife automatic crusher, weighed, and treated with HCl at 1.0 mol L^{-1} (1:15, w/v) for 1 h under stirring at 90 °C, for the removal of minerals. The residue containing chitin and insoluble protein remains were filtered and treated with NaOH at 1.0 mol L^{-1} (1:10) for 2 h under stirring at 70 °C to remove proteins. This final residue was filtered and washed up to the neutralization of chitin, CT.

2.3. Preparation of CS

The extracted CT was weighed and treated with 40% NaOH/$NaHB_4$ (0.250 g of $NaHB_4$ and 300 mL 40% NaOH) under stirring for 30 min at 110 °C to induce CT deacetylation. The solid was filtered and washed several times until pH was adjusted to 7.0 ± 0.2. Using this reaction time (30 min), it was obtained a deacetylation degree (DD) of 62%. Higher reaction times were also used and the following DD (in %) were obtained: 75 (60 min); 92 (120 min); 93 (180 min or 240 min) [17,21].

2.4. Determination of the deacetylation degree of CS

The deacetylation degree of CS was determined by ^1H NMR spectroscopy. ^1H NMR spectra of CS were taken on a Varian spectrometer model Oxford 300 operating at 300 MHz. CS was dissolved in CD_3COOD. The deacetylation degree of CS was calculated using Eq. (1), which correlates the area corresponding to the signal of the hydrogen bound to CH_3 groups (A_{CH_3}) to the area attributed to the hydrogen bound to the carbon-2 of the glucosamin groups (A_{H_2}) [17,21].

$$\%\overline{DD} = \left(\frac{A_{CH_3}}{3A_{H_2}}\right) \times 100 \quad (1)$$

2.5. Analysis of CS and CT morphologies by scanning electron microscopy (SEM)

The CS and CT morphology assays were conducted with a Shimadzu scanning electron microscope model SS 550 operating at 12 keV. SEM micrographs of pure CS particles with the same granulation used in adsorption experiments (300–425 μm) were obtained. Before the examination by SEM, the samples were frozen in liquid nitrogen and lyophilized at −60 °C for 24 h.

2.6. Determination of adsorbed and remaining in solution metals

The adsorption performances of CT and CS for Pb^{2+} and Ni^{2+} were evaluated by square-wave voltammetry. An Auto Lab Pgstat 30 potentiostat/galvanostat (GPES) was used for electrochemical measurements. The amount of heavy metals adsorbed onto CT and CS and remaining in solution were determined using a system of three electrodes constituted of a mercury drop as a working electrode versus Ag/AgCl as a reference electrode and graphite as the counter electrode. The metal concentrations were determined by an analytical curve. In this procedure, solutions with 20.0 mL of electrolyte and 100 μL of metals were used in each determination.

2.7. Adsorption experiments for Pb^{2+} and Ni^{2+} onto CT and CS

Solutions of 100 mg L^{-1} Pb^{2+} and 100 mg L^{-1} Ni^{2+} were prepared from metallic nitrate (Merck) using MilliQ water for dilution. Adsorption experiments were performed by adding 50-mL standard solutions of Pb^{2+} and Ni^{2+} each to a flask with either 50 mg chitin or 30 mg chitosan. The pH was adjusted with the addition of the required volume of a 1.0 mol L^{-1} NaOH

solution to reach basic pH or the addition of the required volume of a 1.0 mol L^{-1} HCl solution to reach acid pH. This was done under stirring at 200 rpm and 25 °C. The adsorbate-to-adsorbent (mg g^{-1}) ratio was obtained by the difference between the initial and final masses of metal in solution [22,23] for each gram of either CT or CS. These procedures were performed with CT and CS particles from 300 to 425 μm in size as determined by granulometric analysis. In the study conditions, CS remained insoluble.

3. Results and discussion

3.1. Determination of CS morphology by scanning electron microscopy

The morphology of CS with deacetylation degree of 75% and molar mass (M_W) of 5.9×10^6 g mol^{-1} was investigated by SEM images [24,25]. In studies of Ni^{2+} and Pb^{2+} ion adsorption onto solid adsorbents, the pore size structure must be considered because this parameter may be an indicative of binding capacity. The metallic ions are lead into the adsorbent basically through diffusion process driven by chemical interactions between metallic ions and adsorbent active sites [24,25].

The SEM micrographs shown in Fig. 1a and b correspond to solid CS. It should be highlighted that solid CS has a tight but porous structure, which could aid in the adsorption process. In this sense, we can speculate that the adsorption of metallic ions onto CS could occur either by pore-penetration or by molecular-level interactions among CS amine groups and metallic ions.

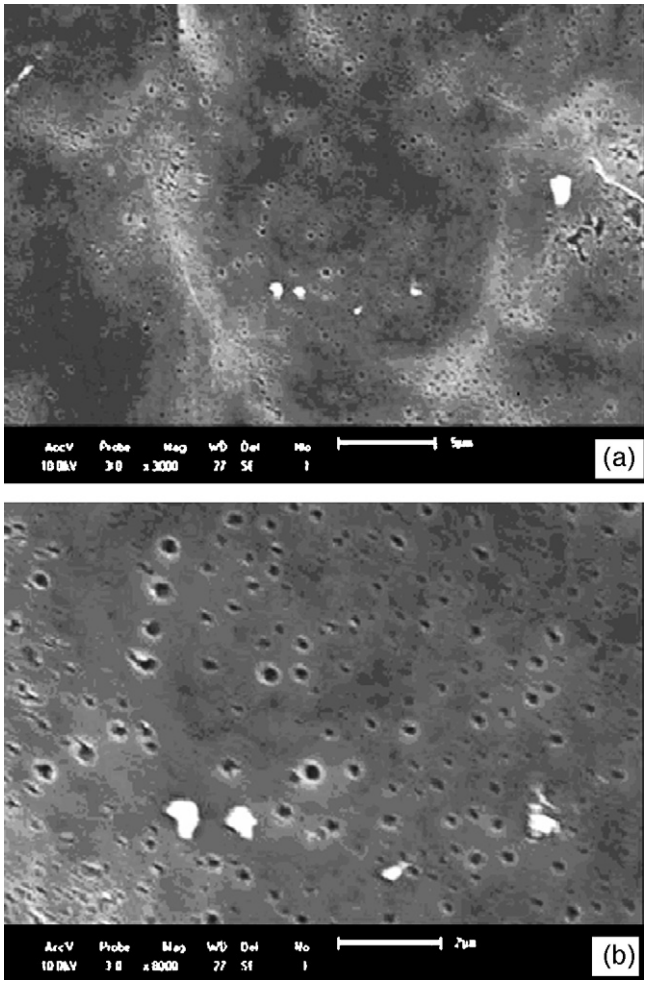

Fig. 1. SEM images of CS after 75% deacetylation. Sub-parts (a) and (b) refer to solid CS.

3.2. The effect of pH on adsorptions studies

Fig. 2 shows the precipitation of Pb^{2+} and Ni^{2+} in aqueous solutions by pH changes. The amounts of 100 mg L^{-1} Pb^{2+} solutions, and 100 mg L^{-1} Ni^{2+} solutions were prepared in MilliQ water using powder metallic nitrate (Merck). The pH changes were performed by adding the required volume of either NaOH or HCl solutions as described earlier. At high pH, the metallic ions bind to hydroxide ions forming $Pb(OH)_2$ and $Ni(OH)_2$ compounds, which are solid at room temperature (close to 25 °C). In Fig. 2, it is observed that the pH threshold for Pb^{2+} is 5.5 and the pH threshold for Ni^{2+} is 7.5. To avoid precipitation and for good binding capacity, the adsorption experiments with Pb^{2+} and Ni^{2+} solutions were conducted at pH from 4.5 to 5.5.

Fig. 3 shows the amounts of Pb^{2+} and Ni^{2+} adsorbed onto CS as a function of pH. The initial concentrations of Pb^{2+} ion solution and Ni^{2+} ion solution were 100 mg L^{-1} for both metals and the adsorption time was set at 24 h. In acidic medium, CS does not show a significant binding capacity for Pb^{2+} and Ni^{2+}. The authors have attributed this effect to the preferential interactions between H^+ ions in solution and the basic NH_2 groups of CS. As most NH_2 groups of CS are in NH_3^+ form, it does not allow binding with metals. In addition, the binding capacity decreased. On the other hand, it was observed a significant enhancement in binding capacity at high pH for both metals up to the threshold pH. As pH increased, interactions between H^+ and NH_2 are destabilized, leading to an improvement of the adsorption of Pb^{2+} and Ni^{2+} onto CS because the NH_2 groups are available for interactions. However, above the threshold pH,

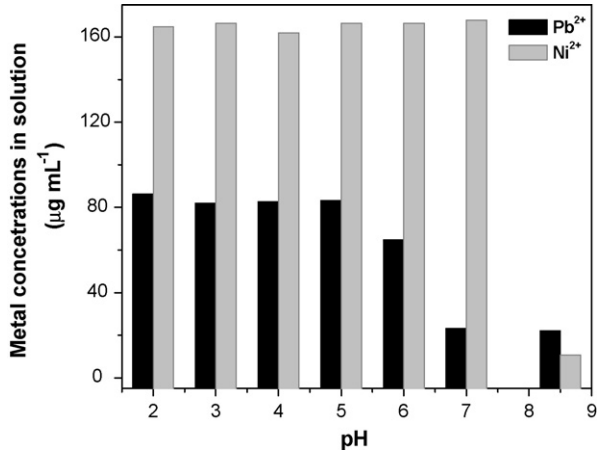

Fig. 2. Effect of pH changes on the precipitation of Ni^{2+} and Pb^{2+} in aqueous solution.

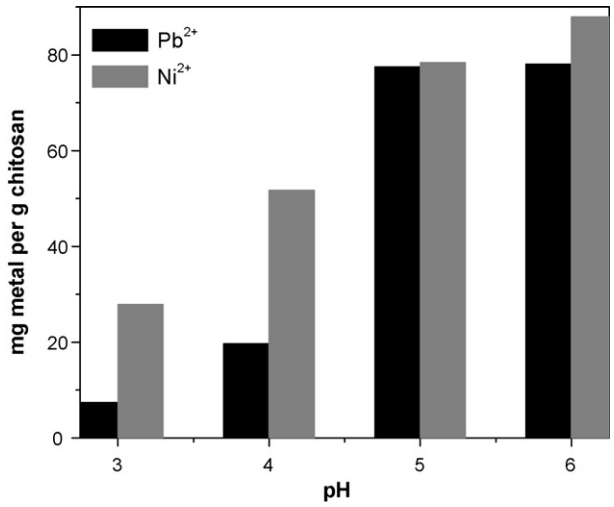

Fig. 3. Effect of pH changes on the adsorption of Pb^{2+} and Ni^{2+} onto CS. The experimental parameters were; 75% deacetylation degree, particle size from 300 to 425 μm, and contact time of 24 h.

the binding capacity decreased because of the precipitation of the metallic ions as hydroxides.

3.3. CT-metal adsorption kinetics curves

Fig. 4 shows the bindings capacities of Pb^{2+} and Ni^{2+} onto CT as a function of time. The initial concentrations of Pb^{2+} and Ni^{2+} were 100 mg L^{-1}. The binding capacities of CT for either Pb^{2+} or Ni^{2} after 48-h contact time were (in mg of ion per g of CT) 32.01 and 61.17, respectively. These values were attributed to two main factors; the large ionic size of Pb^{2+} and the steric hindrance due to the presence of CT acetyl groups. Both factors hinder the molecular arrangement of Pb^{2+} within the CT structure. Other less important factors that might also be considered are the coordination number, aggregation, different complex properties, hydrolysis constants and electrostatic forces [26,27].

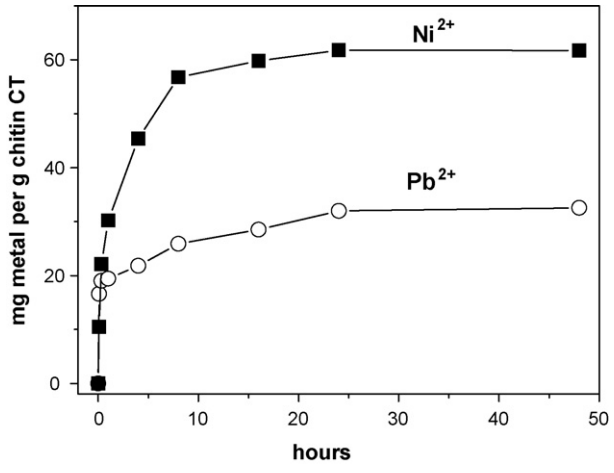

Fig. 4. Adsorption of Pb^{2+} and Ni^{2+} onto CT versus time. The experimental parameters were; pH 4.50, particle size from 300 to 425 μm.

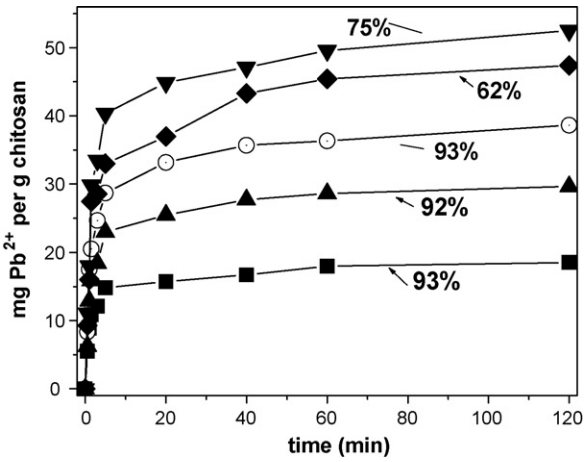

Fig. 5. Effect of CS deacetylation degree on Pb^{2+} adsorption. The experimental parameters were; pH 4.50 and particle size from 300 to 400 μm.

3.4. Effect of the deacetylation degree on the adsorption of Pb^{2+} and Ni^{2+}

Fig. 5 shows the effect of the deacetylation degree of CS on Pb^{2+} adsorption. The initial concentrations of Pb^{2+} and Ni^{2+} were 100 mg L^{-1} for both metallic solutions. High Pb^{2+} adsorption was observed for a deacetylation degree of 75%. Quantitatively, the binding capacity was 50 mg Pb^{2+} per g CS. When the deacetylation degree was kept low (62%), it was observed a reduction in the binding capacity of CS. In this case, a smaller number of amine groups in polymer are generated, resulting in less adsorption. High deacetylation degree does not lead to an improvement of Pb^{2+} binding. Long deacetylation reaction time induces high deacetylation degree; however, it also induces polymer degradation, resulting in chains with low average molecular weight. The polymer chains with either low molecular weight and/or its fragments are released from the coiled structure of CS to the surrounding liquid, affecting the adsorption capacity of CS drastically.

The effect of the deacetylation degree of CS on Ni^{2+} adsorption is shown in Fig. 6. The best binding of Ni^{2+} was detected for deacetylation degree close to 92%. On the order hand, CS adsorbs Ni^{2+} less effectively than Pb^{2+}. The binding capacity of Ni^{2+} onto CS is close to 17 mg g^{-1} after 240 min of contact. The binding effect of Ni^{2+} onto CS observed may be attributed to different interactions among amine groups from different polymer chains as shown in Fig. 7. However, the interactions between Ni^{2+} and amine groups are less established than the interactions between Pb^{2+} and amine groups. An improvement in Ni^{2+} adsorption may be obtained when β-CS is used, because the formation of the complex CS–Ni is more suitable in this molecular arrangement. In β-CS, the NH_2 groups are packed in a parallel molecular arrangement throughout its polymer chains, which favors the formation of strong interactions between CS and Ni^{2+} better. However, in this work, α-CS, the most abundant form, was used [17]. It presents NH_2 groups packed in an antiparallel molecular arrangement throughout its polymeric chains [28]. A schematic drawing of the complex formed by Ni^{2+} and NH_2 groups of α-CS is shown in Fig. 7.

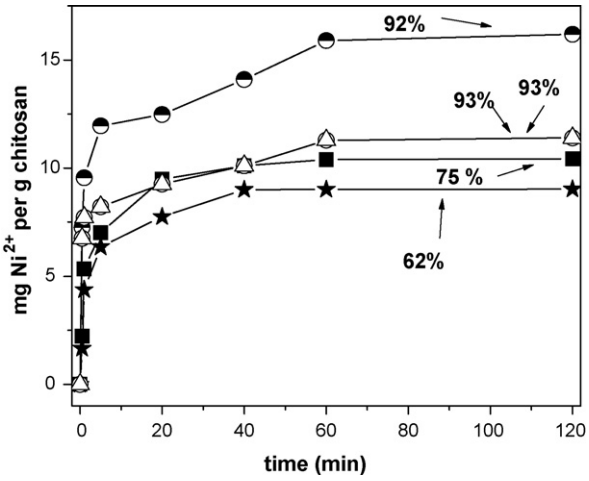

Fig. 6. Effect of CS deacetylation degree on Ni^{2+} adsorption. The experimental parameters were; pH 4.50 and particle size from 300 to 400 μm.

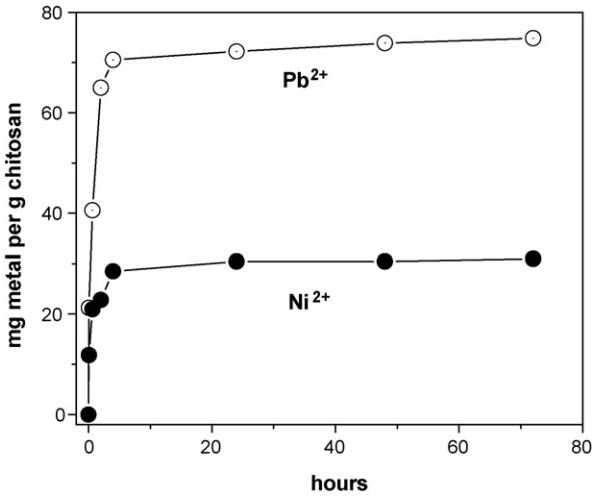

Fig. 8. Binding capacity of Pb^{2+} and Ni^{2+} onto CS in optimal study conditions. The experimental parameters were; pH 5.0, particle size from 300 to 425 μm.

3.5. Adsorption capacity in optimal study conditions

Fig. 8 shows the binding capacity curves of Pb^{2+} and Ni^{2+} onto CS in optimal deacetylation degree, 75% and 92%, respectively. The initial concentrations of Pb^{2+} and Ni^{2+} were 100 mg L^{-1} for both ions. It was observed that CS adsorbed more Pb^{2+} than Ni^{2+} in the time range studied. If CS with 75% deacetylation degree is used, the adsorption values are 74.97 mg g^{-1} of CS for Pb^{2+} and 32.14 mg g^{-1} of CS for Ni^{2+}. Although Pb^{2+} ion has a molecular mass higher than that of Ni^{2+}, this parameter must be minimized by the high porosity of the CS structure, as shown in Fig. 1a and it does not affect adsorption. When porous CS is in contact with either Ni^{2+} or Pb^{2+} solutions, both adsorbates penetrate into the polymer structure throughout the pores easily and the adsorptions for Pb^{2+} and Ni^{2+} are supported by interactions between metallic ions and the active groups of the polymeric chains. The decrease in pore size of CT and CS could affect mostly the adsorption of Pb^{2+} rather than of Ni^{2+} due to the ionic radii.

3.6. Langmuir and Freundlich equilibrium isotherms

Equilibrium isotherms are used to determine the bioadsorbent capacity for metallic ions. The bioadsorbent was stirred with fixed volumes of metal ion solutions varying the initial concentrations in the equilibrium time. The relation between the amount of adsorbed metal and the metal ion concentration remaining in solution is described by the isotherm. Langmuir and Freundlich adsorption isotherms describe the interaction in two different

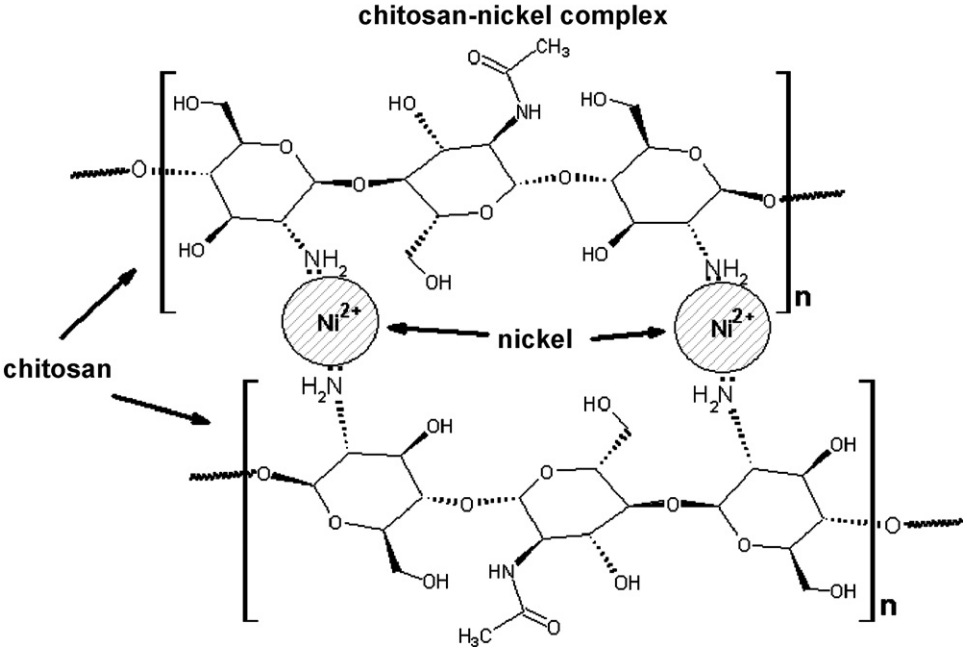

Fig. 7. Schematic representation of the complex of Ni^{2+} ions and CS NH_2 groups with polymeric structure of α-spatial conformation.

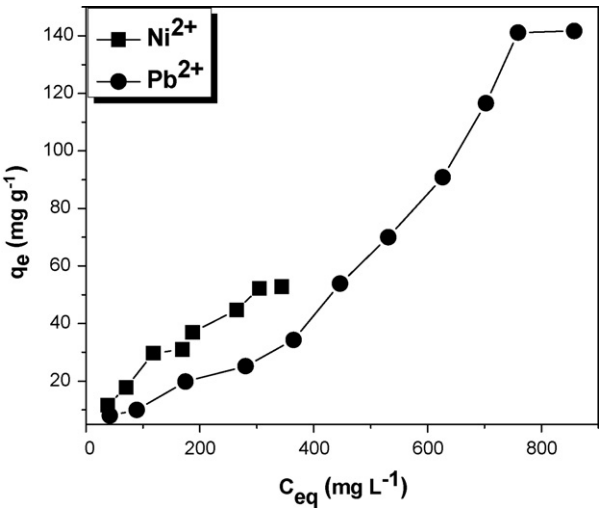

Fig. 9. Adsorption isotherms for CS—Pb and CS—Ni. The experimental parameters were; 75% deacetylation degree, particle size from 300 to 425 μm, pH 5.0, contact time of 24 h and temperature of 20 ± 0.2 °C.

ways; (i) the Langmuir isotherm assume that the adsorption occurs in monolayer or may only occur in a fixed number of definitive localized sites on the surface, and that each site may adsorb only one molecule (monolayer). All sites are equivalent and no interaction may be observed between adsorbed moieties and adjacent molecules. The Langmuir isotherm considers that the energies and enthalpy resulting from the adsorption phenomenon are the same. The equation for this isotherm is represented by:

$$\frac{C_e}{q_e} = \frac{1}{k_L} + \frac{\alpha_L}{k_L} C_e \quad (2)$$

where k_L, α_L are the characteristic constants of the Langmuir equation. The Langmuir equation is based on the assumption that a plot of C_e/q_e versus C_e gives a straight line with slope α_L/k_L and intercepts $1/k_L$ for a structurally homogeneous adsorbent. In this sense, k_L/α_L gives the theoretical monolayer saturation capacity (Q_0). (ii) The Freundlich isotherm is another form of the Langmuir approach for adsorption onto amorphous surfaces. The amounts adsorbed are the summation of all sites. This isotherm describes the reversible adsorption and it is not restricted to a monolayer formation. The Freundlich model is considered as a multi-site adsorption when the surface of the adsorbate is heterogeneous. This model is the most important multi-site adsorption isotherm for heterogeneous surfaces. The equation is represented by:

$$\ln q_e = \frac{1}{n} \ln C_e + \ln k_F \quad (3)$$

where k_F and n are characteristic constants of the Freundlich equation and may be determined by linear fitting. C_e is the concentration of the adsorbent in equilibrium, q_e is the adsorption capacity of the adsorbate and $(1/n) = b$.

The adsorption isotherms for CS–Pb and CS–Ni are shown in the Fig. 9, while the linear replots from Langmuir and Freundlich analysis are shown in Fig. 10a and b for CS–Pb and

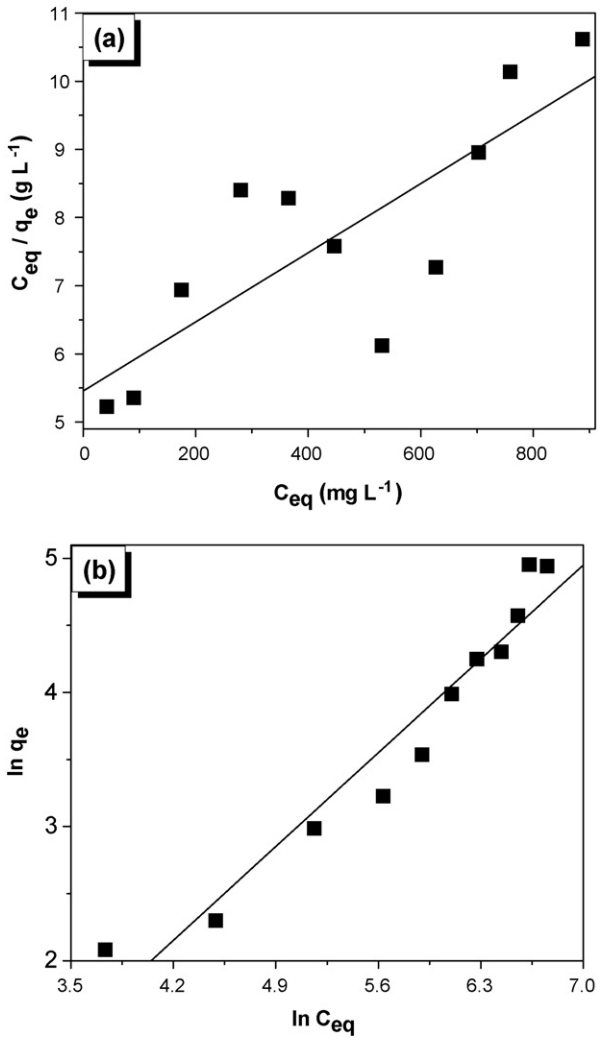

Fig. 10. (a) Langmuir and (b) Freundlich replots of Pb^{2+} adsorption onto CS. The experimental parameters were; 75% deacetylation degree, particle size from 300 to 425 μm, pH 5.0, contact time of 24 h, and temperature of 20 ± 0.2 °C.

in Fig. 11a and b for CS–Ni. The linear replots were evaluated by correlation coefficients (R^2) obtained from plots of Figs. 10 and 11, and Eqs. (2) and (3) considering the isotherm constants. The isotherm constants studied were q_e, α_L, k_L, n, Q_0, b_F and k_F, which are summarized in Table 1. The best

Table 1
Langmuir and Freundlich adsorption isotherms for the Pb^{2+} and Ni^{2+} onto CS-BM

Metal	R^2	α_L (L mg^{-1})	k_L (L g^{-1})	Q_0 (m g^{-1})
Langmuir isotherm				
Pb^{2+}	0.7319	0.00130	0.1954	150.42
Ni^{2+}	0.9136	0.00637	0.4160	65.31
Metal	R^2	b_F	k_F	n
Freundlich isotherm				
Pb^{2+}	0.9677	0.9996	1.9750	1.0004
Ni^{2+}	0.9148	0.5366	2.0852	1.8636

Experimental conditions: pH 5.0';temperature = 20 ± 0.2 °C; particles size = 300–425 μm; contact time = 24 h.

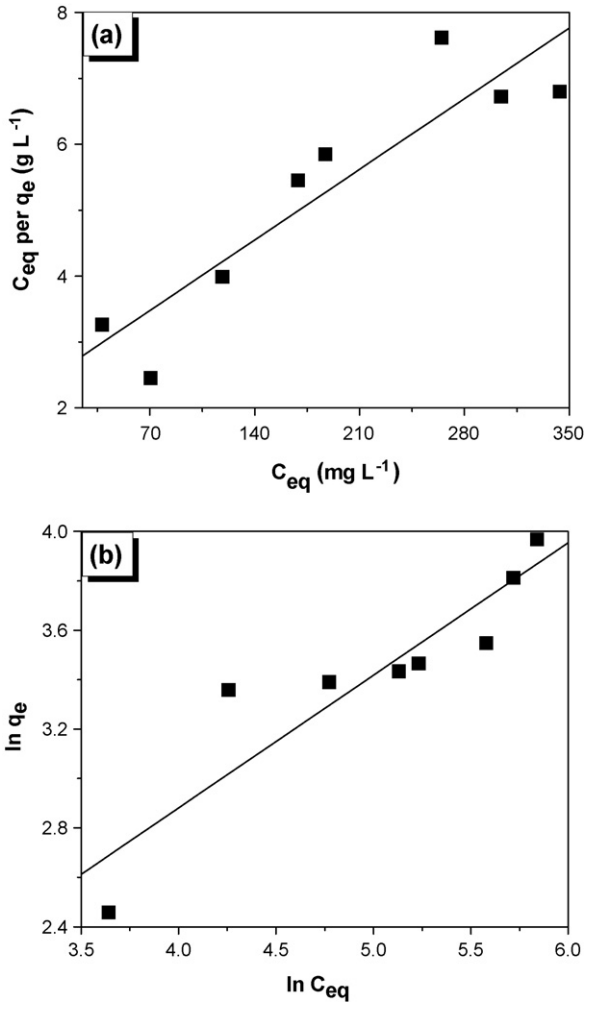

Fig. 11. (a) Langmuir and (b) Freundlich replots of Ni^{2+} adsorption onto CS. The experimental parameters were; 75% deacetylation degree, particle size from 300 to 425 μm, pH 5.0, contact time of 24 h and temperature of 20 ± 0.2 °C.

conditions for the isotherms studied were pH 5.0, temperature 20 ± 0.2 °C, particles size from 300 to 425 μm, 75% deacetylation degree, and equilibrium time of 24 h. The maximum binding capacities of CS–Pb and CS–Ni from the adsorption isotherms shown in Fig. 9 are 141.10 and 52.86 mg g^{-1}, respectively. However, the maximum binding capacity of CS–Pb and CS–Ni estimated from Langmuir replots are 156.67 mg g^{-1} for CS–Pb and 86.51 mg g^{-1} for CS–Ni. The differences between the maximum binding capacities estimated from Langmuir replots are 11.0% for CS–Pb and 65.7% for CS–Ni. From Figs. 10a to 11a, it is observed that the Q_0 values from the Langmuir isotherm of CS–Pb and CS–Ni are 150.42 and 65.31, respectively. The binding equilibrium constant (k_L) values for CS–Pb and CS–Ni are 0.1954 and 0.4160, respectively. The Q_0 values increased in the order $Pb^{2+} > Ni^{2+}$ while the k_L values increase in opposite order. The Langmuir isotherm supported a two-fold increase of k_L values from Pb^{2+} to Ni^{2+} and Q_0 values increased as much as 2.5 from Ni^{2+} to Pb^{2+}. Therefore, as the k_L and Q_0 values are quite different for each type of metallic ions, it is suggested that the data are fitted by the Langmuir equation better than by the Freundlich equation. Taking into account that the k_L values obtained from the Langmuir studies for each CS-metal system are statistically different, it confirmed that Pb^{2+} and Ni^{2+} interact differently with CS. From the R^2 data obtained from the Langmuir model, it is suggested the metal-CS adsorption increases in the following order; CS–Ni > CS–Pb. Different adsorption enthalpies might affect these data. The k_F parameter values for CS–Pb and CS–Ni obtained from Figs. 10b to 11b are 1.975 and 2.085, respectively, and the R^2 values are 0.9687 and 0.9148, respectively. The n values for the CS–Pb and CS–Ni systems are 1.0004 and 1.8636, respectively, and the b_F parameters for CS–Pb and CS–Ni are 0.9996 and 0.5366. As the k_F parameter is different for each CS-metal and the n values are both higher than 1, either electrostatic interaction or ion-exchange or a combined mechanism of metal adsorption onto CS is supported.

In previous studies by Krajewska, it was recognized that the affinity of chitosan to transition metals depends on parameters such as the total concentration of amino groups (deacetylation degree), the availability of these groups (geometrical configuration of chitosan matrix, either α or β or γ), diffusion rate, and matrix water content. The sequence of affinity for metal adsorption onto chitosan was in the order Cu > Hg > Cd > Ni > Pb [26]. On the other hand, the sequence for metallic ion removal by adsorption onto CS considered in this study was in the order Pb > Ni. The different result was due to the larger pore size structure of CS and the ensuing better diffusion process. In addition, CS has a α-configuration and presents NH_2 groups packed in an antiparallel molecular arrangement throughout its polymeric chains [17]. This chitosan conformation supports less binding for Ni^{2+} than for Pb^{2+}. In this way, CS has a good performance mainly in adsorption studies of Pb^{2+} comparatively to either chitosan from crustaceous or other adsorbents [13–14,27], because of its structure and the physical and chemical characteristics are satisfied. It was observed that in comparison to other adsorbents, the chitosan used here had a good performance for Pb^{2+} and Ni^{2+}.

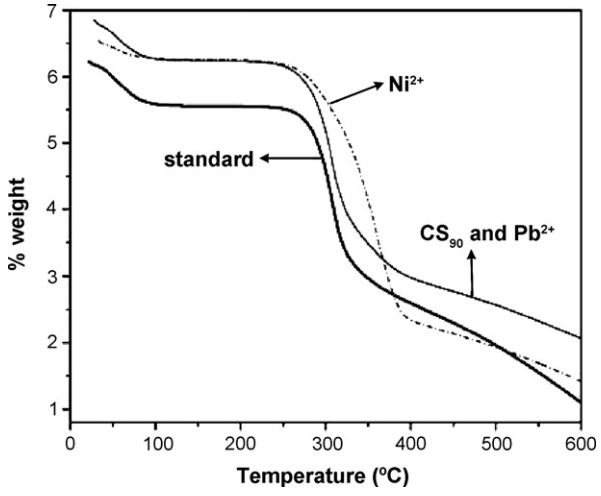

Fig. 12. TGA curves of standard chitosan, CS with 75% deacetylation degree and CS after adsorption of Pb^{2+} and Ni^{2+} at pH 5.0.

3.7. Thermo gravimetric analysis (TGA)

TGA curves of CS 75% (DD), CS after binding to either Pb^{2+} or Ni^{2+} and for the standard CS (92% DD) used as a reference in this analysis are shown in Fig. 12. It was observed two degradation stages for CS regardless of DD or the presence of adsorbed ions. The first begins at 90 °C with 6% weight loss and the second starts at 300 °C, reaching maximum degradation at 350 °C. In the CS-metallic ions systems, the first stage begins at 90 °C with 7% weight loss and the second stage begins at 300 °C with maximum degradation at 400 °C. Thus, the presence of ions in the CS structure induces a better thermal stability compared to that of pure CS. Also, it is important to report that the thermal behavior of CS was in the same profile of standard chitosan.

4. Conclusions

- The adsorption experiments of CT as a reference were conducted and compared with results of CS 75% deacetylated and M_W of 5.9×10^6 g mol^{-1}.
- The binding capacities of CT were 32.01 mg g^{-1} for Pb^{2+} and 61.24 mg g^{-1} for Ni^{2+}. This was attributed to two main factors; the large ionic size of Pb^{2+} and the steric hindrance due to presence of acetyl groups in CT.
- CS with 75% deacetylation degree exhibited a good binding for Pb^{2+} but it adsorbed Ni^{2+} less efficiently.
- From the adsorption isotherms, the maximum binding capacities of CS were 141.10 mg g^{-1} for CS–Pb and 52.86 mg g^{-1} for CS–Ni. The values estimated from Langmuir replots were 156.67 and 86.51 mg g^{-1} for CS–Pb and CS–Ni, respectively. The differences between the adsorption isotherm values and the Langmuir replots were 11.0% for CS–Pb and 63.7% for CS–Ni.
- CS exhibited a good performance principally in adsorption studies of Pb^{2+}.
- As the k_L values and Q_0 were different for each metal, it was confirmed that Pb^{2+} and Ni^{2+} interacted with CS in different ways.
- By analysis of the k_F parameters and for n values to be higher than 1 for the two CS-metals, either electrostatic interaction or ion-exchange or a combined adsorption mechanism of metals onto CS was supported.
- The thermal behavior of CS with deacetylation degree 75% was in the same profile of the standard chitosan.

Acknowledgements

ATP thanks Coordenação de Aperfeiçoamento de Pessoal de Nível Superior (CAPES-Brazil) the doctorate fellowship; AVR, ECM and JN are grateful to Conselho Nacional de Desenvolvimento Científico e Tecnológico (CNPq-Brazil) and Fundação Araucaria-PR (Brazil) for the financial support; MRG and EBT are grateful to the Fundação de Amparo a Pesquisa do Estado de São Paulo (FAPESP-Brazil) for the post-doctorate fellowship.

References

[1] K.N. Dietrich, P.A. Succop, R.L. Bornchein, K.M. Kraft, O. Berger, P.B. Hammond, C.R. Buncher, Lead exposure and neurobehavioral development in later infancy, Environ. Health Perspect. 89 (1990) 13–19.
[2] G.W. Goldstein, Lead poisoning and brain cell function, Environ. Health Perspect. 89 (1990) 91–94.
[3] A.T. Paulino, J.A.A. Tessari, E.M. Nogami, E. Lenzi, J. Nozaki, Lipid increase induced by lead accumulation in tilapia *Oreochromis niloticus*, Bull. Environ. Contam. Toxicol. 75 (2005) 42–49.
[4] E. Merian, M. Anke, M. Ihnat, M. Stoeppler, Metals and their compounds in the environment: occurrence, in: Analysis and Biological Relevance, John Wiley & Sons, New York, 2004.
[5] T.-W. Tan, B. Hu, H. Su, Adsorption of Ni^{2+} on amine-modified mycelium of penicillium chrysogenum, Enzym. Microb. Technol. 35 (2004) 508–513.
[6] C.R.T. Tarley, S.L.C. Ferreira, M.A.Z. Arruda, Use of modified rice husks as a natural solid adsorbent of trace metals: characterisation and development of an on-line preconcentration system for cadmium and lead determination by FAAS, Microchem. J. 77 (2004) 163–175.
[7] K. László, J. Tóth, Characteristic adsorption functions and the surface structure of solid adsorbents, J. Colloid Interface Sci. 286 (2005) 425–432.
[8] K. Abidin, H. Ali, Adsorption of zinc from aqueous solutions to bentonite, J. Hazard. Mater. 125 (2005) 183–189.
[9] P. Catalfamo, A. Ileana, P. Patrizia, C. Francesco, Efficiency of a zeolitized pumice waste as a low-cost heavy metals adsorbent, J. Hazard. Mater. 134 (2006) 140–143.
[10] E. Pehlivan, S. Cetin, B.H. Yanık, Equilibrium studies for the sorption of zinc and copper from aqueous solutions using sugar beet pulp and fly ash, J. Hazard. Mater. 135 (2006) 193–199.
[11] O. Arzu, E. Mehmet, Cu^{2+}, Cd^{2+} and Pb^{2+} adsorption from aqueous solutions by pyrite and synthetic iron sulphide, J. Hazard. Mater. 137 (2006) 626–632.
[12] T. Gotoh, K. Matsushima, K.I. Kikuchi, Preparation of alginate–chitosan hybrid gel beads and adsorption of divalent metal ions, Chemosphere 55 (2004) 135–140.
[13] S.E. Bailey, T.J. Olin, R.M. Bricka, D.D. Adrian, A review of potentially low-cost sorbents for heavy metals, Water Res. 33 (1999) 2469–2479.
[14] S. Babel, T.A. Kurniawan, Low-cost adsorbents for heavy metals uptake from contaminated water: a review, J. Hazard. Mater. B97 (2003) 219–243.
[15] N. Ben-Shalom, N. Kudabaeva, M. Borisover, Copper-binding efficacy of water-soluble chitosans: characterization by aqueous binding isotherms, Chemosphere 59 (2005) 1309–1315.
[16] J. Lerivrey, B. Dubois, P. Decock, G. Micera, J. Urbanska, H. Kozlowski, Formation of D-glucosamine complexes with Cu(II), Ni(II) and Co(II) ions, Inorg. Chim. Acta 125 (1986) 187–190.
[17] A.T. Paulino, J.I. Simionato, J.C. Garcia, J. Nozaki, Characterization of chitosan and chitin produced from silkworm chrysalides, Carbohydr. Polym. 64 (2006) 98–103.
[18] A.J. Varma, S.V. Deshpandea, J.F. Kennedy, Metal complexation by chitosan and its derivatives: a review, Carbohydr. Polym. 55 (2004) 77–93.
[19] E. Guibal, Interactions of metal ions with chitosan-based sorbents: a review, Sep. Purif. Technol. 38 (2004) 43–74.
[20] G.A.F. Roberts, Chitin Chemistry, Macmillan, Houndmills, 1992.
[21] J.I. Simionato, A.T. Paulino, J.C. Garcia, J. Nozaki, Adsorption of aluminium from wastewater by chitin and chitosan produced from silkworm chrysalides, Polym. Int. 55 (2006) 1243–1248.
[22] J.C.Y. Ng, W.H. Cheung, G. Mckay, Equilibration studies of the sorption of Pb(II) ions onto chitosan, Chemosphere 52 (2003) 1021–1030.
[23] J.C.Y. Ng, W.H. Cheung, G. Mckay, Equilibration studies of the sorption of Cu(II) ions onto chitosan, J. Colloid Interface Sci. 255 (2002) 64–74.
[24] R.A.A. Muzzarelli, F. Tanfani, G. Scarpini, G. Laterza, The degree of acetylation of chitins by gas chromatrography and infrared spectroscopy, J. Biochem. Biophys. Methods 2 (1980) 299–306.
[25] R.H. Chen, H.-D. Hwa, Effect of molecular weight of chitosan with the same degree of deacetylation on the thermal, mechanical, and permeabil-

ity properties of the prepared membrane, Carbohydr. Polym. 29 (1996) 353–358.
[26] B. Krajewska, Diffusion of metal ions through gel chitosan membranes, React. Funct. Polym. 47 (2001) 37–47.
[27] A.T. Paulino, F.A.S. Minasse, M.R. Guilherme, A.V. Reis, E.C. Muniz, J. Nozaki, Novel adsorbent based on silkworm chrysalides for removal of heavy metal from wastewater, J. Colloid Interface Sci. 301 (2006) 479–487.
[28] J. Synowiecki, N.A. Al-Khateeb, Production, properties, and some new applications of chitin and its derivatives, Crit. Rev. Food Sci. Nutr. 43 (2003) 145–171.